# REPORT DOCUMENTATION PAGE

Form Approved OMB NO. 0704-0188



| 1. REPORT DATE (DD-MM-YYYY) | 2. REPORT TYPE | 3. DATES COVERED (From - To) |
|---|---|---|
| | New Reprint | - |

4. TITLE AND SUBTITLE

Kinetics of monolayer and bilayer nanoparticlefilm formation during electrophoreticdeposition

5a. CONTRACT NUMBER
W911NF-12-1-0047

5b. GRANT NUMBER

5c. PROGRAM ELEMENT NUMBER
206022

6. AUTHORS

A. J. Krejci, T. Gebre, C. A. Ruggiero, M. D. Mochena, J. H. Dickerson

5d. PROJECT NUMBER

5e. TASK NUMBER

5f. WORK UNIT NUMBER

7. PERFORMING ORGANIZATION NAMES AND ADDRESSES

Florida A&M University
1700 Lee Hall Drive
400 Foote-Hilyer Admin Center
Tallahassee, FL 32307 -6600

8. PERFORMING ORGANIZATION REPORT NUMBER

9. SPONSORING/MONITORING AGENCY NAME(S) AND ADDRESS (ES)

U.S. Army Research Office
P.O. Box 12211
Research Triangle Park, NC 27709-2211

10. SPONSOR/MONITOR'S ACRONYM(S)
ARO

11. SPONSOR/MONITOR'S REPORT NUMBER(S)
60533-CH-REP.5

12. DISTRIBUTION AVAILIBILITY STATEMENT

Approved for public release; distribution is unlimited.

13. SUPPLEMENTARY NOTES

The views, opinions and/or findings contained in this report are those of the author(s) and should not contrued as an official Department of the Army position, policy or decision, unless so designated by other documentation.

14. ABSTRACT

The kinetics of electrophoretic deposition are studied for the growth of monolayers and bilayers of y10 nm iron oxide nanoparticles. The net deposited nanoparticle film is measured as a function of time for five voltages through analysis of scanning electron microcopy images of the films. The collected data suggest that films deposited at different voltages have different kinetic behaviours. Additionally, we observe monolayer and bilayer growth separately, from which we assert that the initiation of the bilayer may be the source of variation in kinetic behaviour

15. SUBJECT TERMS

Electrophoretic deposition, Directed assembly, Iron oxide, Monolayer, Time-resolved

| 16. SECURITY CLASSIFICATION OF: | | | 17. LIMITATION OF ABSTRACT | 15. NUMBER OF PAGES | 19a. NAME OF RESPONSIBLE PERSON |
|---|---|---|---|---|---|
| a. REPORT | b. ABSTRACT | c. THIS PAGE | | | Mogus Mochena |
| UU | UU | UU | UU | | 19b. TELEPHONE NUMBER 850-599-3470 |

**Report Title**

Kinetics of monolayer and bilayer nanoparticlefilm formation during electrophoreticdeposition

**ABSTRACT**

The kinetics of electrophoretic deposition are studied for the growth of monolayers and bilayers of y10 nm iron oxide nanoparticles. The net deposited nanoparticle film is measured as a function of time for five voltages through analysis of scanning electron microcopy images of the films. The collected data suggest that films deposited at different voltages have different kinetic behaviours. Additionally, we observe monolayer and bilayer growth separately, from which we assert that the initiation of the bilayer may be the source of variation in kinetic behaviour.

# REPORT DOCUMENTATION PAGE (SF298)
# (Continuation Sheet)

Continuation for Block 13

ARO Report Number 60533.5-CH-REP
Kinetics of monolayer and bilayer nanoparticlefil...

Block 13: Supplementary Note


Approved for public release; distribution is unlimited.

# Kinetics of monolayer and bilayer nanoparticle film formation during electrophoretic deposition

**A. J. Krejci[1,2], T. Gebre[3], C. A. Ruggiero[4], M. D. Mochena[3] and J. H. Dickerson*[1,2,4,5]**

The kinetics of electrophoretic deposition are studied for the growth of monolayers and bilayers of ~10 nm iron oxide nanoparticles. The net deposited nanoparticle film is measured as a function of time for five voltages through analysis of scanning electron microcopy images of the films. The collected data suggest that films deposited at different voltages have different kinetic behaviours. Additionally, we observe monolayer and bilayer growth separately, from which we assert that the initiation of the bilayer may be the source of variation in kinetic behaviour.

**Keywords:** Electrophoretic deposition, Directed assembly, Iron oxide, Monolayer, Time-resolved

***This article is part of a special issue on Electrophoretic deposition of ceramics: fundamentals and applications***

## Introduction

Electrophoretic deposition (EPD), a versatile, scalable, and rapid process used to fabricate thin films from colloidal suspensions, is an attractive materials casting approach for industrial applications.[1–8] However, the utility of EPD could be dramatically enhanced if a more complete model that describes EPD was to exist. Some models exist that attempt to predict the amount of deposition as a function of time.[9,10] Additionally, functional forms have been found to fit the electrophoretic current profile measured during deposition using a constant voltage.[11] The vast majority of these models involve the EPD of materials suspended in polar solvents, which have notably different kinetics from that of nonpolar solvent suspensions, such as those employed in this study.[9,12] A few studies have examined the notable characteristics of the deposition kinetics of nonpolar solvent EPD.[11,13] However, no model currently exists that satisfactorily describes the EPD process in nonpolar solvent environments.

In this article, we are motivated to execute the initial component of an (semi-)empirical model of the time-resolved deposition of nanoparticles by EPD. We present experiments to measure the time dependence of the quantity of deposition for different deposition voltages. Two aspects of the EPD system used in this study engender simple conditions that should facilitate the development of such an EPD model. First, we used nonpolar solvents to suspend the nanoparticles.[11,14–16] By using nonpolar solvents, we eliminate many of the complexities encountered when using polar solvents, such as electrohydrodynamic flows and electrolysis.[17,18] Second, we can easily deposit monolayer and bilayer nanoparticle films.[11,14,15,19] By using such thin films of nanoparticles, we can ignore the resistive and capacitive effects the film has on the current profile of the system.[9] These simplifications establish an appropriate and reasonable starting point for the development of an EPD model.

## Experimental

Iron oxide nanoparticles were synthesised using previously described procedures.[14,16,20] The nanoparticles were suspended in hexane at a concentration of 0·1 mg $mL^{-1}$; the suspension preparation was facilitated by centrifugation based cleanings.[11,21] The particle size was measured to be $9{\cdot}8 \pm 0{\cdot}9$ nm under transmission electron microscopy using a Phillips CM20 operating at 200 kV (Fig. 1*a*). The nanoparticle films were deposited onto rectangular, epi-ready, doped Si wafers that act as the field-emanating substrate during EPD (Fig. 1*b*). The wafers, cut to a size of $3{\cdot}5 \times 0{\cdot}9$ cm, were mounted in parallel plate capacitor configuration with a 5 mm gap. The wafers were then inserted ~2·8 cm into the nanoparticle suspension (Fig. 1*c*). After insertion, a voltage was applied across the two substrates. Then, the substrates were extracted from the suspension in ~5 mm segments in a stepwise manner. These stepwise extractions occurred after 10, 32, 100, 316 and 1000 s of deposition, corresponding to the first time step through the fifth time step respectively (Fig. 1*d*). The final extraction completely removed the wafers from the NP suspension. The voltage remained on for 60 s while the suspension

[1]Department of Physics and Astronomy, Vanderbilt University, Nashville, TN 37235, USA
[2]Vanderbilt Institute for Nanoscale Science and Engineering, Vanderbilt University, Nashville, TN 37235, USA
[3]Department of Physics, Florida A&M University, Tallahassee, FL 32307, USA
[4]Center for Functional Nanomaterials, Brookhaven National Laboratory, Upton, NY 11973, USA
[5]Department of Chemistry, Vanderbilt University, Nashville, TN 37235, USA

*Corresponding author, email jdickerson@bnl.gov


Published by Maney on behalf of the Institute
Received 2 April 2013; accepted 1 October 2013
DOI 10.1179/1743676113Y.0000000124

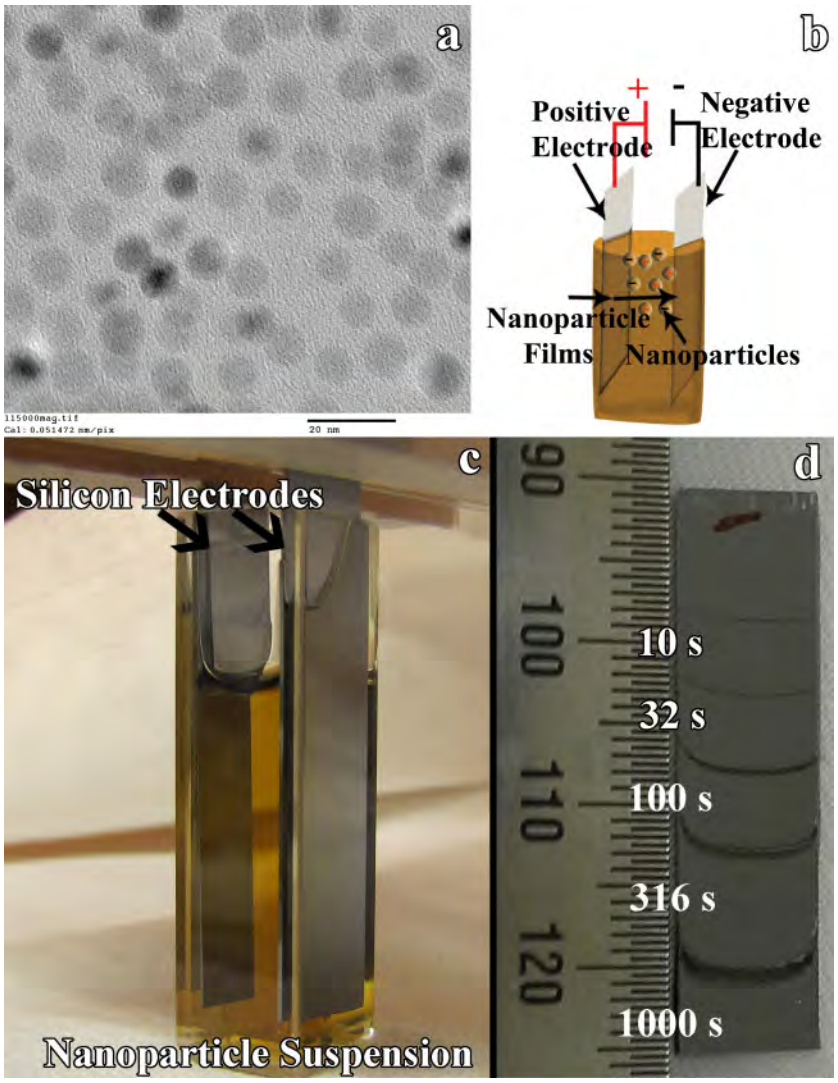


**1** ***a*** **transmission electron microscope image of iron oxide nanoparticles.** ***b*** **schematic of electrophoretic deposition system.** ***c*** **image of execution of EPD experiment. Long silicon electrodes were inserted into a tall, glass container filled with the iron oxide nanoparticle suspension.** ***d*** **photograph that shows wafer after deposition. The dark lines that divide the regions are left by the meniscus during deposition. The wafer is labelled at the top as the negative electrode. The labelled scale is in millimetres**

completely evaporated from the surface.[7,22–24] The above procedure was performed for five voltages chosen on a logarithmic scale: 1, 3·16, 10, 31·6 and 100 V; these correspond to applied electric fields of 2, 6·32, 20, 63·2 and 200 V $cm^{-1}$.

After the deposition, the films were imaged using scanning electron microscopy (SEM). The SEM images reveal three thicknesses of deposition: bilayer thickness, monolayer, and no deposition (voids).[19] To discern among the three components of this film (the substrate, the monolayer and the bilayer), we performed an analysis of the image by segmenting the image into distinct regions into which the locations of each nanoparticle were mapped. This image segmentation process was performed by applying a series of image processing filters to each SEM image. An explicit description of the details of this analytical process, which the authors developed and which is beyond the scope of this article, can be found elsewhere.[21]

Figure 2*a* shows an image of the nanoparticle film that is representative of the samples that were acquired. The darkest regions of this image correspond to bare silicon regions on the sample. Said regions of the silicon substrate can be perceived in very small voids between nanoparticles in the first monolayer as well as in a region, highlighted by the red ovals (a larger bare region). The majority of the SEM image comprises the first monolayer of the film, seen as grey-scaled, spherically contoured shapes (and the resulting segmented images. The bilayer in the image was represented by the brightest spherical shapes. Figure 2*b* depicts regions within the monolayer that consist of voids whose dimensions are larger than the diameter of one nanoparticle. These voids were indicated as black regions, whereas the white regions represent the extant monolayer. Figure 2*c* distinguishes the bilayer (white regions) from the monolayer and voids (black regions). The bilayer was surmised based on the increased intensity that the bilayer nanoparticles exhibited under the SEM imaging conditions. Utilising both segmented images, we compiled a complete map of the three distinct regions within the film.

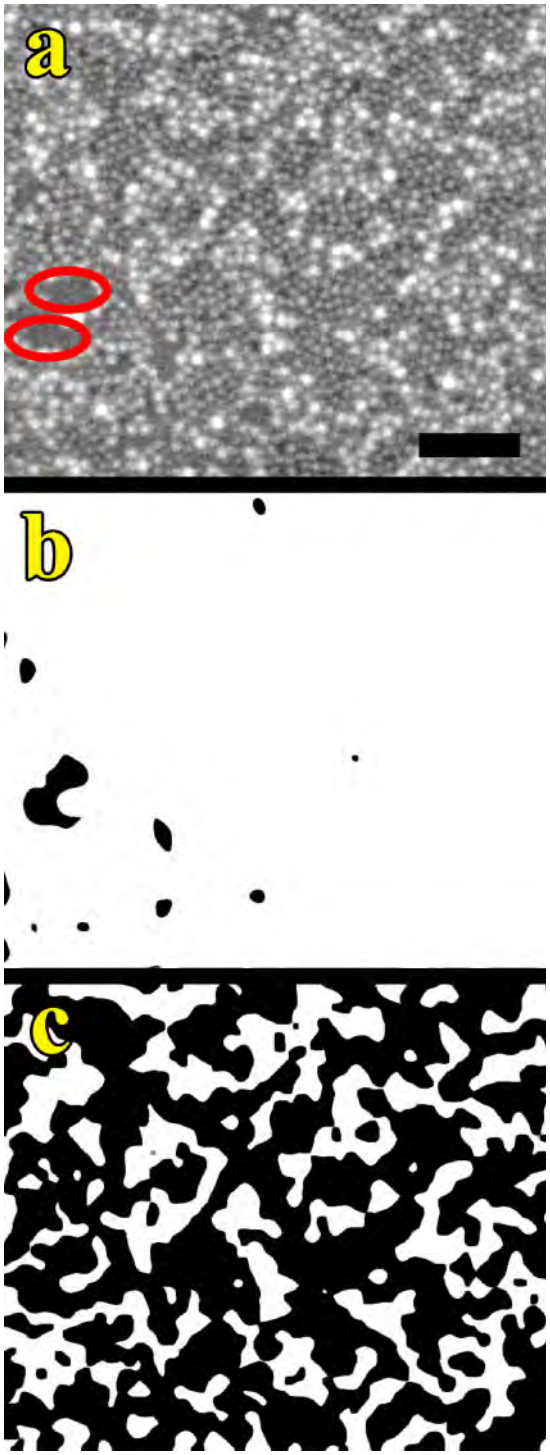


**2 *a* image (SEM) taken of the 100 V sample after 1000 s of deposition. Two large voids are highlighted by red ovals, which encircle them. Scale bar=100 nm. *b* image that displays the result of the monolayer segmentation. White regions are monolayers, whereas black regions are voids in the film. *c* image that displays the result of the bilayer segmentation. White regions represent where the bilayer is located, black regions represent both the monolayer and the voids. By adding the number of white pixels in both images, and dividing by the total number of pixels in one of the images, we obtain the fractional surface coverage for the film[21]**

After segmenting the images, the fractional surface coverage (fsc) was calculated from the sum of (i) the total number of pixels in the image identified as corresponding to nanoparticles within both the monolayer and bilayer ($\text{pixel}_{\text{m\&b}}$) and (ii) the total number of pixels in the image identified as corresponding to nanoparticles within the bilayer ($\text{pixel}_{\text{b}}$), divided by the total number of pixels within the image ($\text{pixel}_{\text{total}}$)

$$\text{fsc} = \frac{(\text{pixel}_{\text{m\&b}}) + (\text{pixel}_{\text{b}})}{(\text{pixel}_{\text{total}})}$$

The average and the standard deviation of the fractional surface coverage, measured from the five images acquired for each voltage and time, were used as the average value and measurement error respectively. Ultimately, fsc can be interpreted as the fraction of the surface that is densely covered by nanoparticles, such that no space exists for additional nanoparticles to deposit. To be clear, fsc does not imply the fraction of the rectilinear surface area that is covered by the spherical nanoparticles, the value of which is limited to ~91% of total coverage based on hexagonally packing of circles in two dimensions. We do mean the surface area that is occupied by the nanoparticles, presuming hexagonal close packing. For example, if nanoparticle film completely covers a substrate, hence forming a monolayer, we would assert that the substrate would be 100% covered. Therefore, the fsc would be 1·0. If a monolayer has formed and a fraction of a bilayer has formed atop the monolayer, say at a fraction of 40%, the fsc would be 1·4 $\text{fsc} = \frac{1{\cdot}0 + 0{\cdot}4}{1{\cdot}0} = 1{\cdot}4$

## Results and discussion

We plotted the fractional surface coverage versus time for the five different voltages measured (Fig. 3*a*). Starting with the 100 V curve, we see that the deposition occurs very rapidly in the beginning. Then, the deposition rate decreases with the deposition ceasing after the fourth time step (316 s). The 31·6 V curve behaves similarly; however, the data indicate that some nanoparticles may still be depositing after 316 s. The 31·6 V sample contains less overall deposition than the 100 V sample, and the results for the 1 and 3·16 V samples also indicate that the deposition begins rapidly and the rate decreases rapidly. Apparently, the nanoparticles continue to deposit during the entire deposition, as the increase in the fractional surface coverage persisted through the experiment.

Finally, we focus more attention on the 10 V sample. The 10 V sample begins similarly to all the other samples; yet, the deposition continues at a high rate even after the fourth time step and deposits just as much as the 31·6 V sample. We investigate this further by separately plotting the growth of the monolayer and the growth of the bilayer (Fig. 3*b* and *c*). In the 10 V sample, the monolayer appears to be completely covering the surface sometime between 136 and 1000 s. The initial components of the bilayer form slowly prior to the 316 s point. Between the fourth and fifth time steps, the deposition of the bilayer markedly increases. Possibly, the completion of the monolayer induces the rapidity of growth of the bilayer. We speculate that when the initial monolayer nears completion, nanoparticles

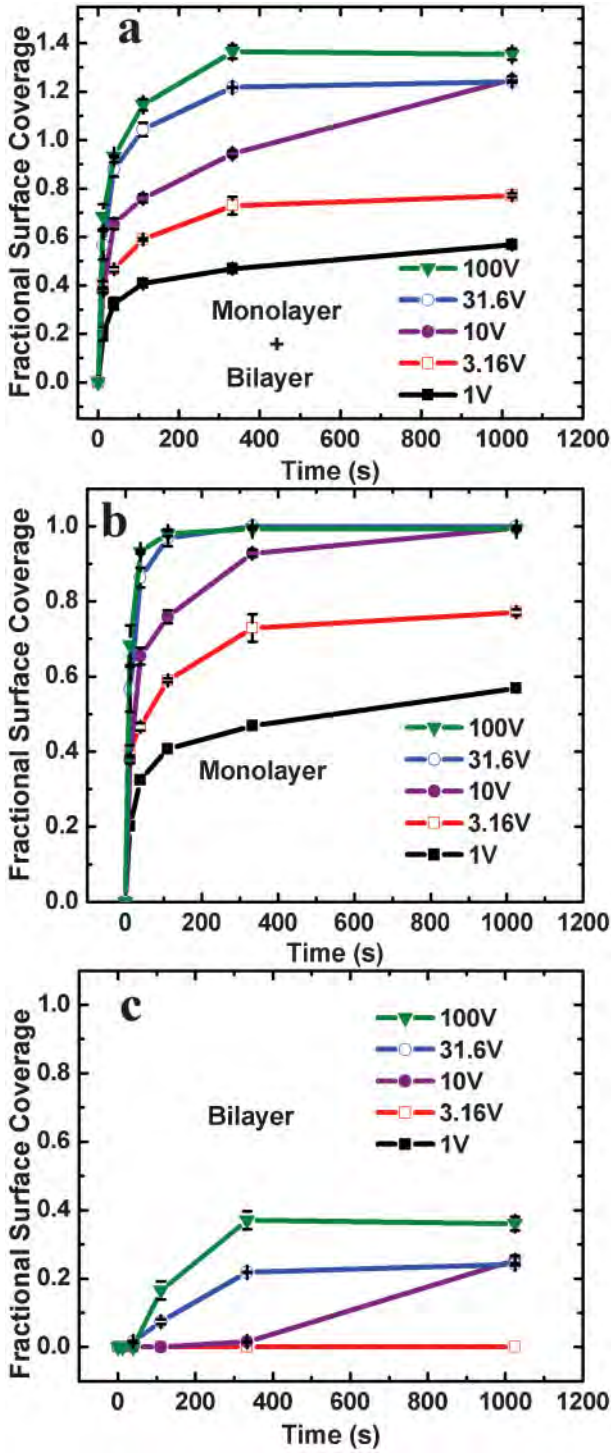


**3** ***a*** **graph of the total fractional surface coverage, fsc, including the coverage comprised by the bilayer and monolayer. Deposition associated with the 100 and 31·6 V samples ceased almost entirely after 316 s. The 10 V sample, deposition continues rapidly during the deposition.** ***b*** **graph that displays the surface coverage from the monolayer only. The 100, 31·6 and 10 V sample all form complete monolayers.** ***c*** **graph that displays the surface coverage from the bilayer only. The 10 V sample bilayer grows rapidly after 316 s of deposition. The bilayer of the 100 and 31·6 V samples nearly ceases to grow after 316 s**

must search for and identify sites on which to deposit. After the monolayer is complete, bilayer particles initially deposit at any location on the surface; thus, they deposit rapidly initially. A time-resolved study (for example with $\leqslant 10$ s intervals) could yield sufficient information to corroborate or to disprove our proposed model. Finally, we note that the bilayer growth does not begin in any of the samples until the fractional surface coverage is $\sim 85\%$. For the two highest voltages, bilayer growth does not occur until after the first time step. Bilayer growth also does not occur at all in the two lowest voltages. This is consistent with previously observed layer-by-layer growth of monolayer films by EPD.[14]

## Conclusion

The fractional surface coverage versus time curve shown herein provide useful information that could be utilised to test the efficacy of EPD models. Thus, we find that the poor time resolution of experiments, such as the one described herein, limits the level of information that can be extracted about the deposition. We envision two possible solutions to the limitations imposed by poor time resolution. First, *in-situ*, 'direct' measurements on the amount of deposition could be done utilising tools, such as an electrochemical quartz crystal microbalance or X-ray scattering measurements. Another possible route to increasing time resolution and repeatability is by acquiring *in-situ*, 'indirect' measurements on the amount of deposition. Measurements, such as suspension concentration versus time that could be determined from absorption measurements, or the current density versus time could be used as indirect measurements. These measurements could then be related to the amount of deposition either by theory or empirical data.

## Acknowledgements

This research is partially supported by the United States Army Research Office, Award W911NF-12-1-0047, and the United States National Science Foundation (NSF) CAREER Award DMR-1054161. Research was carried out at the Center for Functional Nanomaterials, Brookhaven National Laboratory, which is supported by the US Department of Energy, Office of Basic Energy Sciences, under Contract No. DE-AC02-98CH10886.

## References

1. M. Giersig and P. Mulvaney: 'Preparation of ordered colloid monolayers by electrophoretic deposition', *Langmuir*, 1993, **9**, (12), 3408–3413.
2. M. A. Islam, Y. Q. Xia, M. L. Steigerwald, M. Yin, Z. Liu, S. O'Brien, R. Levicky and I. P. Herman: 'Addition, suppression, and inhibition in the electrophoretic deposition of nanocrystal mixture films for CdSe nanocrystals with gamma-$Fe_2O_3$ and Au nanocrystals', *Nano Lett.*, 2003, **3**, (11), 1603–1606.
3. M. A. Islam and I. P. Herman: 'Electrodeposition of patterned CdSe nanocrystal films using thermally charged nanocrystals', *Appl. Phys. Lett.*, 2002, **80**, (20), 3823–3825.
4. S. V. Mahajan and J. H. Dickerson: 'Dielectric properties of colloidal $Gd_2O_3$ nanocrystal films fabricated via electrophoretic deposition', *Appl. Phys. Lett.*, 2010, **96**, 113105.
5. E. M. Wong and P. C. Searson: 'ZnO quantum particle thin films fabricated by electrophoretic deposition', *Appl. Phys. Lett.*, 1999, **74**, (20), 2939–2941.
6. M. Verde, M. Peiteado, A. C. Caballero, M. Villegas and B. Ferrari: 'Electrophoretic deposition of transparent ZnO thin films from highly stabilized colloidal suspensions', *J. Colloid Interface Sci.*, 2012, **373**, (1), 27–33.
7. S. A. Hasan, D. W. Kavich and J. H. Dickerson: 'Sacrificial layer electrophoretic deposition of free-standing multilayered nanoparticle films', *Chem. Commun.*, 2009, **25**, 3723–3725.

8. S. A. Hasan, J. L. Rigueur, R. R. Harl, A. J. Krejci, I. Gonzalo-Juan, B. R. Rogers and J. H. Dickerson: 'Transferable graphene oxide films with tunable microstructures', *ACS Nano*, 2010, **4**, (12), 7367–7372.
9. B. Ferrari, R. Moreno and J. A. Cuesta: 'A resistivity model for electrophoretic deposition', in 'Electrophoretic depositon: fundamentals and applications II', (ed. A. R. Boccaccini et al.), 175–180; 2006, Ütikon, Trans Tech Publications Ltd.
10. P. Sarkar and P. S. Nicholson: 'Electrophoretic deposition (EPD): mechanisms, kinetics, and application to ceramics', *J. Am. Ceram. Soc.*, 1996, **79**, (8), 1987–2002.
11. I. Gonzalo-Juan, A. J. Krejci and J. H. Dickerson: 'Toward dynamic control over $TiO_2$ nanocrystal monolayer-by-monolayer film formation by electrophoretic deposition in nonpolar solvents', *Langmuir*, 2012, **28**, (11), 5295–5301.
12. J. H. Dickerson: 'Electrophoretic deposition of nanomaterials'; 2012, New York, Springer.
13. M. A. Islam: 'Amphoteric CdSe nanocrystalline quantum dots', *Nanotechnology*, 2008, **19**, (25), 255708.
14. A. J. Krejci, I. Gonzalo-Juan and J. H. Dickerson: 'Evolution of ordering in iron oxide nanoparticle monolayers using electrophoretic deposition', *ACS Appl. Mater. Interfaces*, 2011, **3**, 3611–3615.
15. A. J. Krejci, J. Mandal and J. H. Dickerson: 'Patterned substrates to facilitate long-range ordering in the formation of nanoparticle monolayers by electrophoretic deposition', *Appl. Phys. Lett.*, 2012, **101**, (4), 043117–043114.
16. D. W. Kavich, J. H. Dickerson, S. V. Mahajan, S. A. Hasan and J. H. Park: 'Exchange bias of singly inverted $FeO/Fe_3O_4$ core-shell nanocrystals', *Phys. Rev. B*, 2008, **78B**, (17), 174414.
17. P. J. Sides: 'Electrohydrodynamic particle aggregation on an electrode driven by an alternating electric field normal to it', *Langmuir*, 2001, **17**, (19), 5791–5800.
18. M. G. Song, K. J. M. Bishop, A. O. Pinchuk, B. Kowalczyk and B. A. Grzybowski: 'Formation of dense nanoparticle monolayers mediated by alternating current electric fields and electrohydrodynamic flows', *J.Phys. Chem. C*, 2010, **114C**, (19), 8800–8805.
19. A. J. Krejci, C. G. W. Thomas, J. Mandal, I. Gonzalo-Juan, W. He, R. L. Stillwell, J.-H. Park, D. Prasai, V. Volkov, K. I. Bolotin and J. H. Dickerson: 'Using Voronoi tessellations to assess nanoparticle–nanoparticle interactions and ordering in monolayer films formed through electrophoretic deposition', *J. Phys. Chem. B*, 2013, **117B**, 1664.
20. J. Park, K. J. An, Y. S. Hwang, J. G. Park, H. J. Noh, J. Y. Kim, J. H. Park, N. M. Hwang and T. Hyeon: 'Ultra-large-scale syntheses of monodisperse nanocrystals', *Nature Mater.*, 2004, **3**, (12), 891–895.
21. A. J. Krejci, C. G. W. Thomas and J. H. Dickerson: 'Statistical assessment of order within systems of nanoparticles: Determining the efficacy of patterned substrates to facilitate ordering within nanoparticle monolayers fabricated through electrophoretic deposition', *Phys. Rev. E*, 2013, **87E**, (4), 042307.
22. S. A. Hasan, D. W. Kavich, S. V. Mahajan and J. H. Dickerson: 'Electrophoretic deposition of CdSe nanocrystal films onto dielectric polymer thin films', *Thin Solid Films*, 2009, **517**, (8), 2665–2669.
23. S. V. Mahajan, J. Cho, M. S. P. Shaffer, A. R. Boccaccini and J. H. Dickerson: 'Electrophoretic deposition and characterization of Eu(2)O(3) nanocrystal-Carbon nanotube heterostructures', *J. Eur. Ceram. Soc.*, 2010, **30**, (5), 1145–1150.
24. S. V. Mahajan, D. W. Kavich, M. L. Redigolo and J. H. Dickerson: 'Structural properties of electrophoretically deposited europium oxide nanocrystalline thin films', *J. Mater. Sci.*, 2006, **41**, (24), 8160–8165.